The Journal of Molecular Diagnostics, Vol. 14, No. 4, July 2012

http://dx.doi.org/10.1016/j.jmoldx.2012.02.001

A Simple Method for Amplifying RNA Targets (SMART)

Stephanie E. McCalla,* Carmichael Ong,* Aartik Sarma,* Steven M. Opal,†‡ Andrew W. Artenstein,†‡ and Anubhav Tripathi*

From the Center for Biomedical Engineering, School of Engineering and Division of Biology and Medicine, and the Warren Alpert School of Medicine,† Brown University, Providence; and the Department of Medicine and the Center for Biodefense and Emerging Pathogens,‡ Memorial Hospital of Rhode Island, Pawtucket, Rhode Island*

We present a novel and simple method for amplifying RNA targets (named by its acronym, SMART), and for detection, using engineered amplification probes that overcome existing limitations of current RNA-based technologies. This system amplifies and detects optimal engineered ssDNA probes that hybridize to target RNA. The amplifiable probe-target RNA complex is captured on magnetic beads using a sequence-specific capture probe and is separated from unbound probe using a novel microfluidic technique. Hybridization sequences are not constrained as they are in conventional target-amplification reactions such as nucleic acid sequence amplification (NASBA). Our engineered ssDNA probe was amplified both off-chip and in a microchip reservoir at the end of the separation microchannel using isothermal NASBA. Optimal solution conditions for ssDNA amplification were investigated. Although KCl and $MgCl_2$ are typically found in NASBA reactions, replacing 70 mmol/L of the 82 mmol/L total chloride ions with acetate resulted in optimal reaction conditions, particularly for low but clinically relevant probe concentrations (≤100 fmol/L). With the optimal probe design and solution conditions, we also successfully removed the initial heating step of NASBA, thus achieving a true isothermal reaction. The SMART assay using a synthetic model influenza DNA target sequence served as a fundamental demonstration of the efficacy of the capture and microfluidic separation system, thus bridging our system to a clinically relevant detection problem. *(J Mol Diagn 2012, 14:328-335; http://dx.doi.org/10.1016/j.jmoldx.2012.02.001)*

Influenza is a widespread pathogen that results in approximately 36,000 deaths annually in the United States.[1] Influenza comprises a variety of subtypes, which are classified by the antigenic subtype of hemagglutinin (H1 to H16) and neuraminidase (N1 to N9) proteins expressed on the viral particles.[2] Seasonal influenza is generally caused by H1N1, H3N2, and H1N2 viruses,[3] whereas the highly pathogenic avian flu is caused by the H5N1 subtype.[4] Recently, a novel, swine-derived recombinant variant of H1N1 virus resulted in a limited pandemic.[5] A recurrent pandemic of influenza could result in millions of deaths worldwide.[6] Such a catastrophic event could be avoided if rapid point-of-care diagnostics were available to health workers at the source of the infection, such that they could contain the infection before it spreads into the global community.[7,8] Additionally, rapid diagnosis of influenza would prevent excessive antibiotic use, which leads to antibiotic-resistant bacterial strains and is a large financial burden because of the extra cost of otherwise unnecessary treatment, hospitalization, and medication.[9,10]

A number of approaches have been investigated for influenza diagnostics, but each has associated limitations. Viral culture is specific and provides viable virus for further testing,[11] but requires 3 to 14 days for results, limiting its use for rapid diagnostics.[12] Immunospecific tests, such as rapid antigen tests and immunofluorescence microscopy, lack sensitivity and do not provide sequence-specific information for subtyping.[13] Viral nucleic acid amplification and detection can generate subtype or strain-specific information, but these tests are also complex and expensive. PCR requires expensive benchtop thermal cyclers and trained technicians.[12] Nucleic acid sequence-based amplification (NASBA) is faster than PCR for RNA amplification and compares favorably with PCR for HIV RNA detection in clinical samples,[14,15] but it is limited by RNA secondary structure, which makes primer design and multiplexing difficult. Hybridization sites on long, clinically relevant RNA strands require stringent oligonucleotide design, with only a small fraction of sequences hybridizing efficiently to RNA.[16] Poor hybridization of ssDNA oligonucleotides complicates primer design, so that many conserved regions are not successful as NASBA priming sites. To combat these issues, NASBA begins with a 65°C heating step before the addition of enzymes to disrupt full-length RNA secondary structure,[17] and primer sites for NASBA reactions are typically 100 to 250 nucleotides apart, to avoid products with inhibitory secondary structure.[18]

Supported by grants from the National Science Foundation (BES-0555874) and the NIH (1R21 A1073808-01 A1).

Accepted for publication February 9, 2012.

CME Disclosure: The authors of this article and the planning committee members and staff have no relevant financial relationships with commercial interest to disclose.

Address reprint requests to Anubhav Tripathi, Ph.D., Biochemical Engineering Laboratory, Brown University, Box D, Providence, RI 02912. E-mail: Anubhav_Tripathi@brown.edu.

Recently, diagnostic NASBA assays integrated with microfluidic systems have shown improvements over conventional benchtop techniques. These reactors decrease reagent use and further decrease energy consumption of the isothermal system by decreasing the reaction volume. Additionally, the small reaction volumes inherent in microfluidic chips (10 nL to 2 μL) concentrate the target molecule of interest to improve primer binding and reaction kinetics. A preliminary study showed the efficacy of small (10 to 50 nL) reaction volumes in a silicon-glass reaction chamber,[19] followed by use of a reactor containing 10 parallel 80-nL chambers that filled by capillary action.[20] A final reactor design contained 11 parallel channels with two separate chambers for each heating step, separated by hydrophobic burst valves.[21] The second chamber included dehydrated enzymes, which were shown to function in a real-time NASBA reaction on the addition of off-chip heated reagents and primers. Although the full reaction was not run on-chip (the sample was purified off-chip), and although the capillary loading resulted in loss of sample, that study demonstrated several advantages of a microfluidic diagnostic system. The reactor was made to be simple, multiplexed, automated, and shelf-stable and to consume fewer reagents and energy than its benchtop counterpart.[21] Another assay integrated purification and amplification of RNA using a polydimethylsiloxane (PDMS) chamber reactor.[22] Two reactors were contained on one chip, which would allow two RNA samples to be simultaneously purified from bacterial lysate, mixed with reaction mix, heated, mixed with enzyme, and detected real-time using sequence-specific molecular beacons. Both systems show the ability of microfluidics to create a closed, efficient, automated system that can decrease technician time, human error, and potential for contamination. Together, these studies have demonstrated the viability and advantages of incorporating a microfluidic platform with NASBA.

We propose a novel amplification method, SMART (the acronym stands for "simple method for amplifying RNA targets"), that both incorporates the advantages of microfluidics and avoids the limitations of NASBA (including inhibitory secondary structure of the amplified RNA segment and constrained binding sites between 100 and 250 nucleotides apart). SMART achieves this goal by incorporating a binding step and a microfluidic separation step, which allows the two hybridization sites to be located anywhere along the RNA target. Additionally, incorporation of an engineered ssDNA probe allows the user to choose amplifiable probe and primer sequences, which reduces secondary structure and enables the user to optimize reaction kinetics. It is important to note that the amplification step in SMART does not directly amplify the starting RNA.

To demonstrate this novel method, experiments were first performed off-chip to verify that the amplification step created the expected nucleic acid products and to optimize solution conditions. After verification of the optimal amplifiable probe set and solution conditions, the optimal amplifiable probe set and solution conditions were then transferred to the microchip platform to investigate microfluidic separation and amplification. The novel technique investigated in the present study achieved separation of bound probe from free probe by magnetically dragging beads through a microfluidic channel. Optimal real-time amplification and detection of the probe on-chip was also investigated.

The SMART method uses two probes that bind to specific sequences within the target RNA, allowing investigators to test for multiple characteristics of a pathogen, such as subtype, drug resistance, and strain. The major components of the SMART assay are presented in Figure 1. A capture step (Figure 1A) associates bound probe molecules with a magnetic bead by hybridizing target RNA to a capture probe, consequently improving specificity because of the additional binding site needed. The sequence of the two flanking ends of the SMART probe (Figure 1B) can be adjusted by the user to optimize amplification reaction kinetics. Because of the high probe amplification efficiency, separation via a microfluidic chip platform is required to minimize contamination with unbound probe molecules. The assay therefore includes a novel and simple method for separating unbound probe molecules using a PDMS chip and a magnet (Figure 1C). Capture sample is placed in well W1, and unbound probe is separated by holding a magnet to the bottom of the microchip and slowly moving it to well W2, dragging the bead-nucleic acid complex through a large volume of buffer.

Amplification of the probe is performed via NASBA (Figure 1D), starting with the ssDNA amplifiable probe (Figure 1B). As with standard NASBA procedures, two primers are used in conjunction with three enzymes (AMV-RT, T7 RNA polymerase, and RNase H). We demonstrate amplification both on-chip and off-chip (in a tube).

Materials and Methods

Design of Capture Probes, SMART Probes, Primers, and Molecular Beacons

Custom oligonucleotides (Table 1) were purchased from either Integrated DNA Technologies (Coralville, IA) or Eurofins MWG Operon (Huntsville, AL). The probe portion complementary to the H5 RNA target was chosen to be a sequence that has been previously shown to bind to viral RNA (vRNA).[23] Sequences of the nucleic acid arms flanking either side of the complementary portion were chosen to minimize secondary structure. This was done by first using an online folding tool, DINAMelt (DINAMelt Server, RNA Institute, SUNY Albany, Albany, NY; available at *http://mfold.rna.albany.edu*), to reject sequences with predicted excessive secondary structure. The optimal probe and primer set was then chosen by finding the probe that gave the greatest product yield as shown via gel electrophoresis after a 90-minute amplification step.

NASBA Reactions

The NASBA reaction was run in 200-μL polypropylene tubes, in transparent plastic cuvettes, and in 3-mm-diameter PDMS microwells. Reaction volumes varied from 5 to 70 μL. The base NASBA mix contained 40 mmol/L Tris (pH 8.0), 12 mmol/L $MgCl_2$ or $(CH_3COO)_2Mg$ (MgOAc),

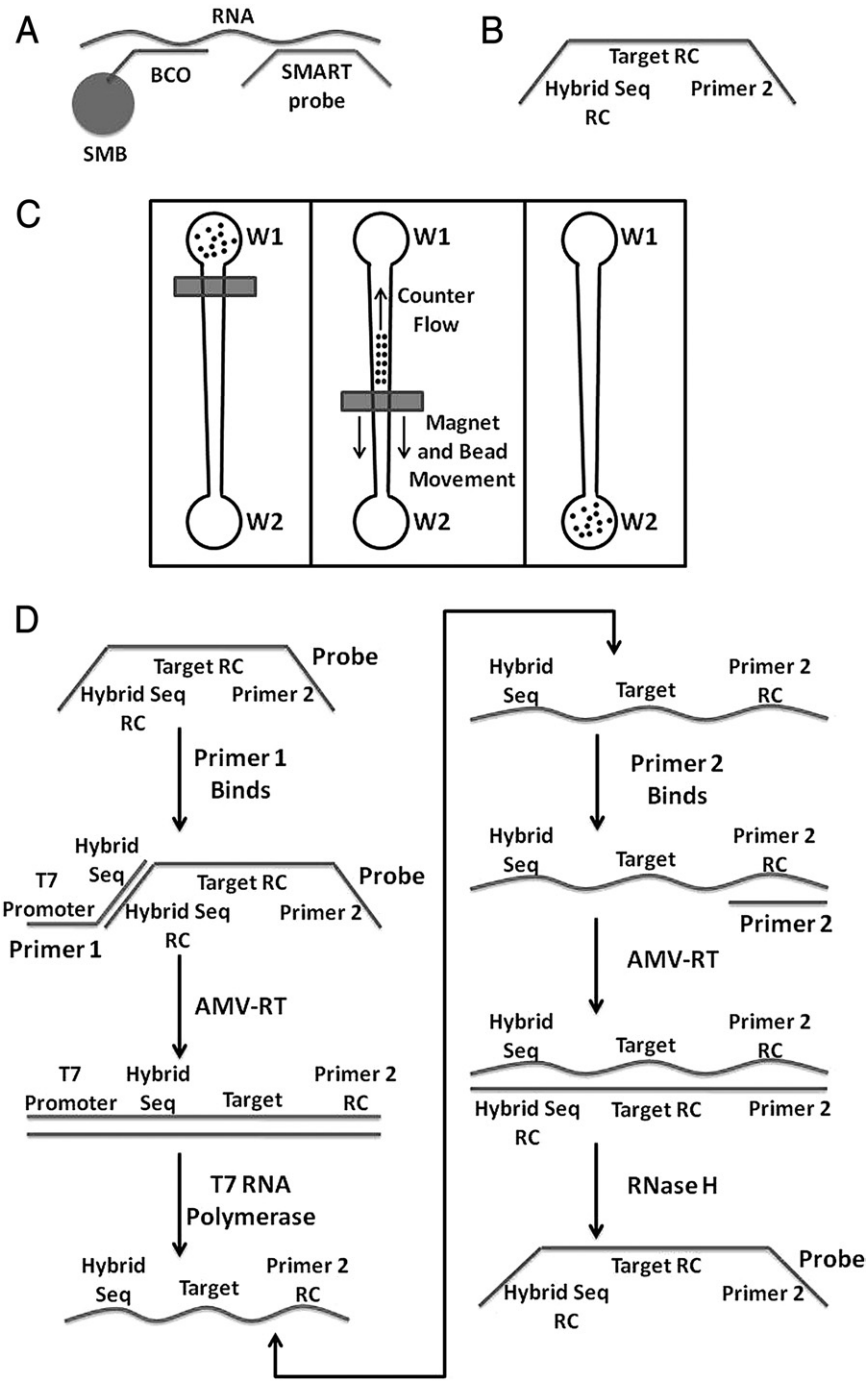

Figure 1. Schematics of the SMART assay. **A:** Capture. Influenza vRNA is captured on magnetic beads (SMB) using a sequence-specific biotinylated oligonucleotide (BCO). An amplifiable probe is also specifically captured on the RNA molecule, and beads are washed to remove unbound probe. BCO, biotinylated capture oligo; SMB, streptavidin-coated magnetic bead. **B:** Probe design. The amplifiable probe includes a central sequence for vRNA hybridization and two ends for primer hybridization designed to minimize probe secondary structure. Seq, sequence; RC, reverse compliment. **C:** Separation step. Beads are placed in well W1, and a magnet is used to move them from the well to the channel. The magnet is then moved toward well W2, moving the beads through a large volume of buffer, effectively separating unbound probe from the capture complex. A counterflow helps this process. Beads are finally deposited in W2 and well mixed before being removed for off-chip amplification or preparation for on-chip amplification. **D:** Probe amplification. The 3′ arm of the probe binds to the first primer, which contains the T7 promoter sequence. AMV-RT elongates primer 1 to create a DNA:RNA hybrid, which is converted to ssDNA by RNase H. Primer 2 binds and is elongated by AMV-RT, creating dsDNA capable of transcription by T7 RNA polymerase. The resulting RNA binds to primer 2 and AMV-RT creates a DNA:RNA hybrid. RNase H degrades the RNA, leaving a copy of the ssDNA amplifiable probe. The reaction is thus cyclic and exponential.

70 mmol/L KCl or CH_3COOK (KOAc), 5 mmol/L dithiothreitol, 1 mmol/L dNTP, 2 mmol/L rNTP, 0.2 μmol/L each primer, and 15% dimethyl sulfoxide at the final reaction concentrations. Real-time amplification reactions also included 50 nmol/L final concentration of molecular beacon. The base enzyme mix contained 1.6 U/μL T7 RNA polymerase, 0.325 U/μL AMV-RT, 0.005 U/μL RNase-H, and 0.105 mg/mL bovine serum albumin (BSA) at the final reaction concentrations. To test optimal solution conditions, additional BSA and polysorbate 20 (Tween 20) were added as indicated. Three different thermal scenarios were used to test optimal heating conditions: heating to 65°C for 5 minutes and cooling to 41°C for 5 minutes before the addition of enzymes, heating to 41°C for 2 minutes before the addition of enzymes, and mixing the reaction mix and enzymes at room temperature before heating to 41°C. Off-chip heating was achieved using a MyCycler thermal cycler (Bio-Rad Laboratories, Hercules, CA) or a water bath housed within a fluorometer (Photon Technology International, Birmingham, NJ). In-well heating was achieved using a Thermal-Clear thin-film heater (14.73 × 55.88 mm^2; Minco, Minneapolis, MN) affixed to the bottom of the microreactor (Figure 2A). NASBA reactions were run at 41°C for 90 minutes, and

Table 1. Oligonucleotides Used in the SMART Method

Oligo	Sequence
Amplifiable probe	5′-TCAAGAGTAGACACAGGATCAGCAT*AGGCAATAGATGGAGTCAC***GTAATCAGATCAGAGCAATAGGTCA**−3′**
Capture probe	/5BioTEG/5′-ATGGTAGATGGTTGGTATGGGTA-3′
Beacon	[6∼FAM] 5′-CGTAGGCAATAGATGGAGTCACTACG-3′ [BHQ1a∼6FAM]
Primer 1 (optimal)	5′-AATTCTAATACGACTCACTATAGGGAGAAGG**TGACCTATTGCTCTGATCTGATTAC**−3′
Primer 1 (alternate)	5′-TAATACGACTCACTATAGG**TGACCTATTGCTCTGATCTGATTAC**−3′
Primer 2	5′-TCAAGAGTAGACACAGGATCAGCAT-3′
ssDNA target-H5	5′-GTGACTCCATCTATTGCCTAAAAAAATACCCATACCAACCATCTACCAT-3′
ssDNA target-H3	5′-ATTCCCTCCCAACCATTTTCTATGAAAAAAAACACATCATAAGGGTAACAGTTGCTG-3′

Probes, primers, and molecular beacon used in the NASBA reactions target H5 vRNA, but for this proof-of-concept work, a short ssDNA synthetic target with H5-binding sites was used. The H3 ssDNA target contains binding sites specific for H3 vRNA, which serves as a negative control for H5 ssDNA target identification. The amplifiable probe sequence is conserved in 93.6% of all sequenced human H5 strains, and the capture probe is conserved in 89.3% of all sequenced human H5 strains. The beacon contains a FAM molecule on the 5′ end and a black hole quencher molecule on the 3′ end. The italicized region in the amplifiable probe corresponds to a binding site in H5 vRNA. Bold regions are the primer 1 binding sites. The underlined region corresponds to the T7 RNA polymerase promoter.

products were detected both in real time by molecular beacon fluorescence and by diluting the sample 1:5 in RNase-free water and running gel electrophoresis (Small RNA kit; Agilent Technologies, Santa Clara, CA).

PDMS Reactor Fabrication

Masks were created using AutoCAD software version 2011 (Autodesk, San Rafael, CA) and negative masks were printed at 20,000 dots per inch (CAD/Art Services, Bandon, OR). Photoresist (SU-8 100; MicroChem, Newton, MA) was spin-coated at a thickness of 120 μm onto silicon wafers [diameter 2 inches (∼5.08 cm)], prebaked at 65°C, soft-baked at 95°C, and exposed to UV light in the presence of the negative mask to selectively cross-link channels. The wafer was then baked again, placed in SU-8 developer to remove non-cross-linked SU-8, and cleaned using isopropanol. The resulting master mold was used to create PDMS microfluidic reactors (Figure 2, A and B). Sylgard 184 elastomer base was mixed 1:10 with curing agent (Dow Corning, Midland, MI), poured over the mask, and cured for 1 hour at 75°C. Holes 3 mm in diameter were punched into the PDMS reactor to form wells. The PDMS reactor and a 1-mm-thick soda-lime glass slide (Corning, Corning, NY) were cleaned with ethanol and treated with plasma for 1 minute 40 seconds using a Harrick 32G plasma cleaner under vacuum [30 in Hg (∼101.59 kPa)] at high radio frequency (Harrick Plasma, Ithaca, NY). The channels were placed face down onto the glass slide, forming an irreversible bond between the plasma-treated glass and PDMS. Baking the PDMS reactor at 70°C for at least 30 minutes after joining appeared to improve the glass-PDMS bond.

Capture of Target Synthetic ssDNA

The short synthetic strand of ssDNA, amplifiable probe (Eurofins MWG Operon), and a biotinylated H5 capture probe (Integrated DNA Technologies) (Table 1) were mixed in a hybridization buffer composed of 20 mmol/L Tris (pH 8.0), 20 mmol/L $MgCl_2$, 150 mmol/L NaCl, 0.02% Tween 20, and 1 mg/mL BSA. A negative control sample contained an ssDNA target specific for H3 vRNA, and a bead control contained only the capture probe. The mixtures were heated to 70°C for 2 minutes and cooled to 4°C for 5 minutes before the addition of 2.8-μm-diameter Invitrogen M-280 magnetic beads (Life Technologies, Carlsbad, CA) for a final volume of 20 μL. The samples were then incubated at room temperature for 35 minutes. Beads were collected at the bottom of the tube using cylindrical neodymium magnets (K&J Magnetics, Jamison, PA), and 18 μL of the supernatant was removed before transfer of the beads to the microfluidic separation platform.

Separation of Probe Complex

Separation of the bead-probe complex (Figure 1A) from free amplifiable probe molecules (Figure 1B) was

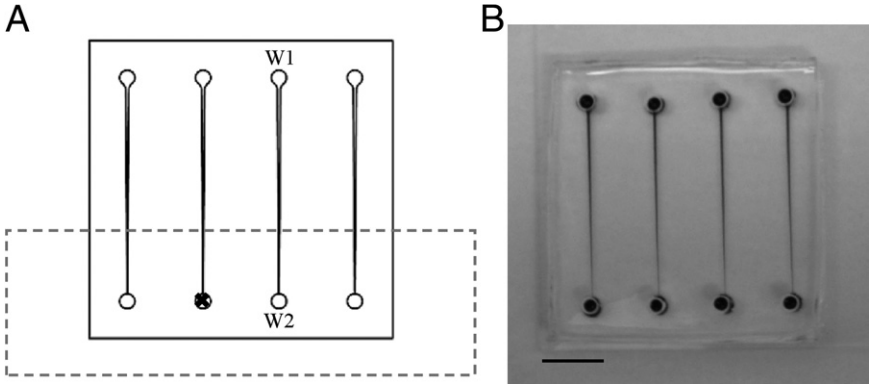

Figure 2. Chip design for microfluidic separation and on-chip amplification. **A:** Schematic of chip design. Beads are placed in well W1, and a magnet is pulled from well W1 to W2, washing unbound probe from the capture complex (Figure 1A). A wider opening at W1 allows beads to enter the channel more easily. **Dashed box** indicate the location of a heating device, and an **X** indicates the thermocouple position; both are used for on-chip amplification temperature control. **B:** Photo of chip. Wells and channels are filled with dye to enhance contrast. Scale bar = 1 cm.

achieved using a custom microfluidic reactor (Figure 2). Reactor cleaning and preparation was achieved by pressurizing the well with a 1-mL syringe, then flushing the channels with nuclease decontamination solution, followed by flushing three times with nuclease-free water (Integrated DNA Technologies, Coralville, IA) and finally flushing two times with priming buffer (1 mg/mL BSA, 0.1% Tween 20). The microchips were stored at 4°C for at least 14 hours. To set up a counterflow, well 2 (W2; Figure 2A) contained 12 μL of priming buffer, well 1 (W1; Figure 2A) contained 2 μL priming buffer, and the chip was held at an approximately 15-degree tilt toward W1. Beads were placed in W1 and moved through the channel by moving a neodymium magnet along the bottom of the channel at $\leq$1 mm/second. When beads were $<$1 cm from W2, the flow was stopped by the removal of solution in both W1 and W2 and the addition of 12 μL of paraffin oil to W1. For off-chip amplification experiments, the solution in W2 was replaced with 5 μL of fresh priming solution. Beads were then pulled into W2, collected in a polypropylene tube, and W2 was rinsed with an additional 6 μL of priming buffer. The beads were then collected at the bottom of the tube and all but 2 μL of solution was removed for downstream NASBA reactions. For on-chip amplification experiments, the solution in W2 was replaced with a NASBA reaction mix that included free probe molecules, and beads were pulled into W2.

In-Well Real-Time Probe Amplification

Real-time amplification of ssDNA probe was conducted in a microwell using NASBA mix without separation, such that the ssDNA probe was included in the NASBA mix and added directly to microwell W2 (Figure 2A). To mimic SMART reaction conditions, in-well probe amplification included beads from a bead control capture reaction and a subsequent separation step as described above. The reactor channel contained priming solution and 12 μL of paraffin oil in W1. The reactor W2 contained 5 μL NASBA mix (after the addition of 0.4 μL sample mix) and 5 μL paraffin oil, to avoid sample evaporation. An adjacent reactor channel contained identical solution conditions and W1 contents, but had 5 μL of priming solution and 5 μL of paraffin oil in W2. A Minco Thermal-Clear thin-film heater (14.73 mm $\times$ 55.88 mm^2) was affixed to the bottom of the reactor and centered under the reactor well and the adjacent well (Figure 2A). A type K thermocouple (Omega Engineering, Stamford, CT) was placed in the adjacent well to accurately determine fluid temperature in the wells. An external power supply (RK-80H; Matsusada Precision, Kusatsu City, Shiga, Japan) provided 4 to 5 V to the heater to achieve 41°C in the well. The reactor was placed under a Nikon Eclipse TE300 fluorescent microscope (Nikon Instruments, Melville, NY) with a blue filter set (450 to 490 nm excitation, 515 nm long-pass emission), a 4$\times$ objective, a photomultiplier detection system with a gain of 700 V (model 814; Photon Technology International, Birmingham, NJ), and an integrated high speed shutter (Melles Griot, Albuquerque, NM) set to open for 0.2 seconds. A custom in-house data acquisition program written using LabVIEW version 8.6 (National Instruments, Austin, TX) collected photomultiplier tube output at a rate of 12 to 15 Hz.

Results

Off-Chip Probe Amplification and Optimization

We first validated that the amplification reaction worked as designed, yielding expected products. To investigate this, combinations of starting material, including amplifiable probe, primers (primer 1 alternate and primer 2; Table 1), and dsDNA, were first characterized by small-RNA gel electrophoresis to find their expected peaks and bands on an electropherogram plot. In addition, the dsDNA was transcribed under NASBA conditions with T7 RNA polymerase to find the expected band for the RNA product. Given this information, a series of tests varying the presence of enzymes with amplifiable probe and primers in NASBA conditions were performed to verify the full NASBA amplification. Three conditions were used: AMV-RT only, both AMV-RT and T7 RNA polymerase, and all three enzymes (Figure 3A). For all conditions, runs were performed using KCl NASBA buffer with a 65°C/41°C heating step before amplification. Analysis was performed using gel electrophoresis. Outcomes of the experiment confirmed that the amplification reaction was occurring as expected (Figure 3A). One important note is that the product contains several peaks of varying length. These peaks are all confirmed to be products, because they appear when the corresponding cDNA is transcribed in NASBA conditions with only T7 RNA polymerase present. We believe that these alternate peaks occur as the polymerase prematurely aborts transcription. This does not affect the detection methods, however, because the beacon targets the middle of the transcribed RNA and thus needs only roughly the first 45 to 50 nt to successfully detect the product. No other nucleic acid species appear within the range of the RNA transcribed. Before we performed the remaining experiments, the primers themselves were modified to yield the maximum product RNA. The resulting primer set was comprised of primer 1 (optimal) and primer 2 (Table 1). These optimal primers were used for the remaining experiments.

A study to inspect the effect of replacing chloride ions with acetate ions was also conducted, to optimize NASBA for our application. To achieve this, an experiment was performed under four amplification conditions and with the base NASBA mix adjusted: i) a positive control; ii) replacing KCl with KOAc; iii) replacing $MgCl_2$ with MgOAc; and iv) replacing both KCl and $MgCl_2$ with acetate complements. Samples were subjected to 65°C/41°C heating steps before amplification, and they were analyzed using gel electrophoresis. Replacing all of the chloride salt with acetate salt increased product yield, but a combination of 70 mmol/L acetate and 12 mmol/L chloride salts yields the optimum balance for these four conditions (Figure 3B).

Because gel electrophoresis allows only for endpoint quantification, the previous result was investigated further to ensure that this method leads to an improvement

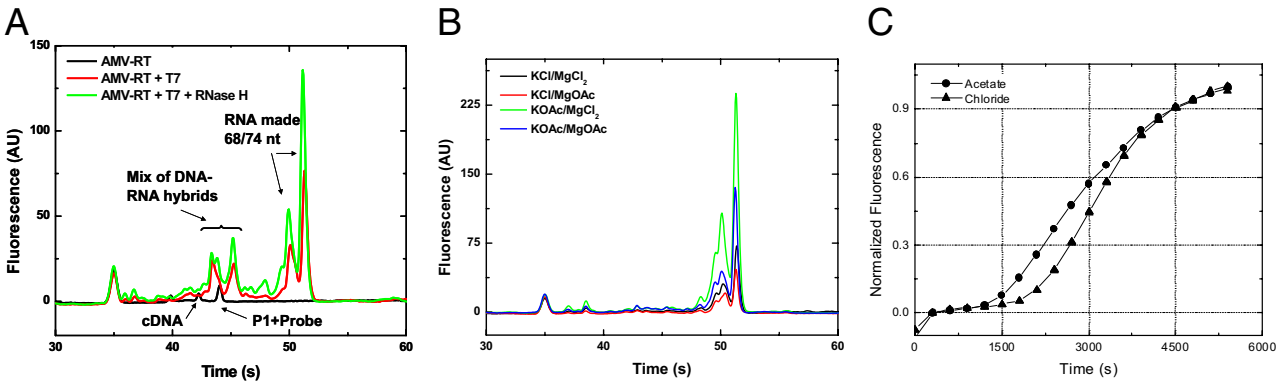

Figure 3. Off-chip probe amplification. **A:** Products made during a NASBA amplification of an engineered ssDNA probe. This electropherogram shows the individual bands (peaks) attributed to each product as enzymes are added to the reaction. The approximate product sizing is extrapolated from the electropherogram of a known small RNA ladder. **B:** Determining the effects of acetate and chloride ions in our NASBA system (100 pmol/L probe). Although the addition of acetate does increase overall product yield, amplification is optimal when a small concentration of chloride ions (12 mmol/L) is retained in the form of $MgCl_2$. **C:** Real-time NASBA of H5 probe on the fluorometer, with the initial 65°C/41°C heating step performed in a thermal cycler. Replacing KCl with KOAc causes a faster initial rising time, but slows the exponential phase of the reaction. AU, arbitrary units.

in real-time detection. A positive control using KCl and an experimental sample replacing KCl with KOAc were prepared. After initial heating steps of 65°C followed by 41°C were performed in a thermal cycler, each sample was run in a fluorometer for a 90-minute amplification reaction. The acetate sample had a faster initial rising time than the chloride sample, even though the chloride sample had a faster exponential phase (Figure 3C). The data support using KOAc in place of KCl, because use of KOAc yields faster results during real-time amplification.

On-Chip Probe Amplification and Optimization

A microfluidic assay for the separation and amplification of bound probe molecules aims to simplify and streamline influenza detection, as well as to save energy and reagents. The removal of the initial 65°C heating step shortens the overall assay time, decreases the energy required to operate the device, and simplifies the heating implement necessary. To determine the effects of removing this initial heating step, optimal H5 probe sequences were amplified under varied heating conditions. A full heat cycle before adding the mix to the well (65°C for 5 minutes and 41°C for 5 minutes before the addition of enzyme) was compared with adding the full NASBA mix to the well at room temperature and heating to 41°C on-chip for 1 pmol/L of probe. A real-time in-well reaction that was exposed to a full heating cycle showed significantly faster exponential kinetics than the reaction that was brought to 41°C from room temperature, although the time to positive did not appear to vary between the two samples (Figure 4A).

The addition of KCl had already been shown to increase the exponential phase of the NASBA reaction (Figure 3C), so reincorporating KCl into the reaction mixture was also studied (Figure 4B). KCl aided amplification without a heating step at 1 pmol/L (3×10^6 copies), but drastically reduced amplification without a heating step at 100 fmol/L (3×10^5 copies). The reincorporation of half

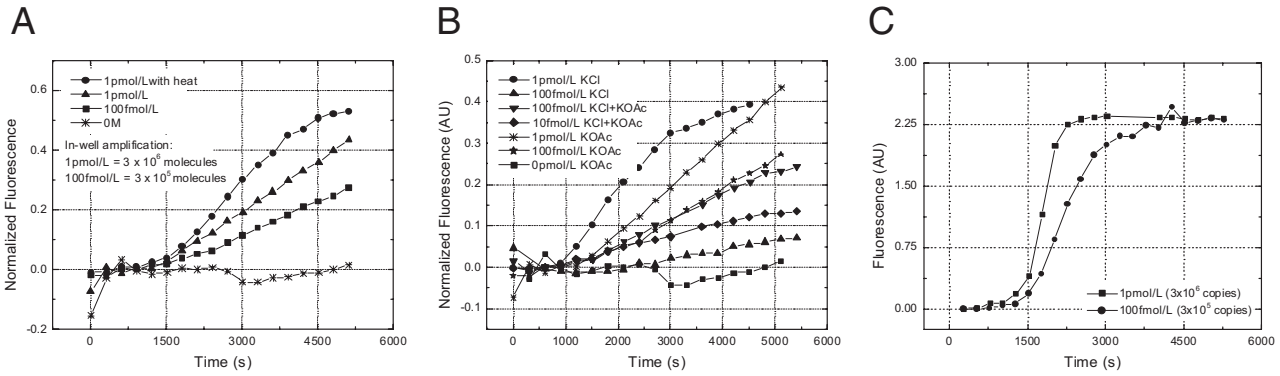

Figure 4. On-chip sensitivity. Molecular beacon fluorescence was monitored over time during real-time probe amplification in the well. Beads were included in the well to mimic SMART conditions, and paraffin oil was placed over the reaction to prevent sample evaporation. **A:** The effect of the 65°C/41°C heating step versus only a 41°C heating step when amplifying H5 probe in real-time in the chip well. Although the extra 65°C step yields a higher endpoint signal, the difference in time to positive is small. **B:** The effect of acetate concentration on real-time probe amplification in the well without the initial 65°C/41°C heating step. The addition of chloride salt is beneficial at high (1 pmol/L) probe concentrations and shows the beginning of a plateau region at 5000 seconds, but it reduces reaction kinetics at lower (100 fmol/L) concentrations. The addition of both 50% KCl and 50% KOAc (35 mmol/L KCl and 35 mmol/L KOAc) yields reaction kinetics similar to those of the pure KOAc system (70 mmol/L KOAc). **C:** Amplification with an initial 41°C heating step, 1 mg/mL additional BSA, and 0.02% Tween-20 gives optimal real-time amplification in the well. The addition of a 41°C heating step before adding enzymes most likely prevents primer-dimer at low probe concentrations, and BSA most likely prevents enzyme adsorption at the oil/water interface.

of the original KCl concentration (35 mmol/L KCl, 35 mmol/L KOAc) did not appear to affect real-time amplification at these levels, and a linear amplification could again clearly be seen for both 1 pmol/L and 100 fmol/L free amplifiable probe. Increasing concentrations of either chloride or acetate ions lead to decreased transcription rates by T7 RNA polymerase, but the polymerase is more sensitive to chloride ions than acetate ions.[24] Because the amplification reaction is cyclical, a decrease in efficiency at any given step is more pronounced at lower concentrations; this could explain the benefit of using KOAc in place of KCl at lower concentrations of initial probe. It may also imply that the change of anion increased the combined efficiency of AMV-RT and RNase H in the steps crucial to the cyclic portion of amplification. In addition, it is possible that nonspecific primer-dimers occur in our system, particularly given the low operational temperature and long priming sequences required. A low, clinically relevant probe concentration with delayed amplification may be inhibited by excessive primer-dimer formation. This is particularly problematic when enzyme mix is added at room temperature. Although amplification can proceed at low probe concentrations if enzymes are added before heating the NASBA mix to 41°C, it may be advantageous to heat the sample to the reaction temperature before the addition of enzymes. These data imply that optimal solution conditions for in-well amplification of low concentration probe molecules include replacing KOAc with KCl.

In-well kinetics may also differ from benchtop reactions, because of the contact of the reaction with PDMS and with paraffin oil. PDMS is the main component of our microfluidic device (Figure 2), and paraffin oil is present to prevent sample evaporation and contamination in the reactor. Proteins have been shown to adsorb to PDMS[25] and at oil/water interfaces,[26] which could sequester enzyme in our system. To determine whether enzyme adsorption adversely affects in-well reaction kinetics, NASBA reactions were performed using an additional 1 mg/mL BSA and 0.02% Tween 20 in the reaction mix. To prevent primer-dimer pairs, the reaction mix was heated to 41°C before the addition of enzymes. Reaction kinetics were aided by the addition of BSA and Tween (Figure 4C), likely because of BSA adsorption to the hydrophobic regions of the PDMS and oil/water interface.

Capture and Amplification of Probe via SMART Assay

After determining optimal reaction conditions for in-well probe amplification, we tested the ability of the system to operate from the capture step to the amplification and detection step. Synthetic H5 ssDNA (1 pmol/L) was captured with 2 pmol/L each of amplifiable probe and capture probe. A negative control reaction contained synthetic H3 ssDNA, and a bead control contained only capture probe (Table 1). After microfluidic separation from free probe molecules, the beads were removed from W2 (Figure 2A) and collected, and all but 2 μL of fluid was removed from the sample. The beads were transferred to a downstream 15-μL NASBA reaction; the bead control received 1 pmol/L total of amplifiable probe, to ensure that the beads and the solution conditions from the microfluidic separation did not inhibit the downstream reaction. A positive control (1 pmol/L amplifiable probe) and negative control (0 pmol/L amplifiable probe) were also run, to ensure that the reaction chemistry was robust. The samples were heated to 65°C and cooled to 41°C before the addition of enzymes, and the reaction was run for 90 minutes. The reactions were quantified on a small-RNA gel electrophoresis chip. The bead control did not differ notably from the positive control. A representative example of the H5 probe amplification after capture, with the electropherogram, is shown in Figure 5. The sample containing the target molecule (H5) contained 7430 pg/μL total product RNA, whereas the sample containing a false target (H3) contained 1155 pg/μL total RNA. The negative control contained no visible product RNA. Although the small peak in the H3 amplification sample indicates nonspecific amplifiable probe adsorption, this small peak corresponds to a late amplification rise in the exponential NASBA kinetics, with a small rise at the end of 90 minutes.

Discussion

Experiments showed that the polymerase prematurely aborts transcription, and thus the SMART method required optimization of primers and buffer components to reduce the population of aborts and to maximize reaction kinetics. As already noted, the detection scheme for influenza RNA was not affected by these aborts. It is important to note that the anions (chloride or acetate) affected the combined efficiency of AMV-RT and RNase H in the amplification. Similarly, addition of enzyme at reaction temperature and adsorption of enzymes to PDMS were important factors in understanding the amplification efficiency. The SMART system was robust at determining

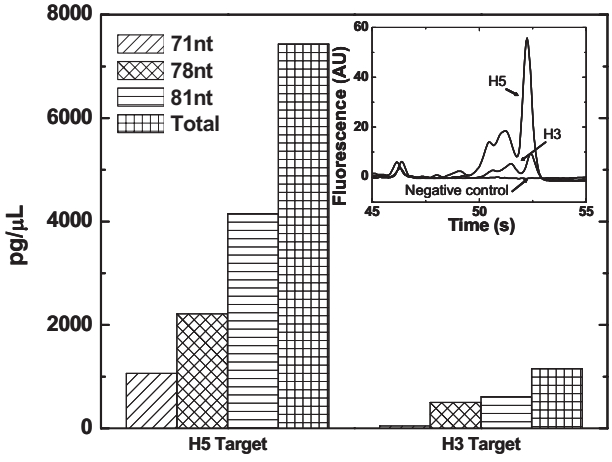

Figure 5. Probe sensitivity with capture of functional RNA (fRNA): Amplification of probe captured in hybridization buffer. The 90-minute amplification of 1 pmol/L (1.2×10^7 copies total) captured fRNA with an original 2 pmol/L free probe concentration, separated on-chip, amplified off-chip, and detected by diluting 1:5 and running on an RNA gel. Although there is a large drop in amplification of the negative control sample, a small peak in the negative control capture electropherogram (**inset**) shows evidence of nonspecific probe adsorption.

the presence of target molecules, particularly when the sample was run for <90 minutes. The nonspecific adsorption may be further decreased by lengthening the separation and washing step by extending the length of the channel or manipulating the solution conditions during capture or separation.

Here, we have demonstrated a novel method for amplification and detection of RNA targets by using amplifiable probes that are engineered to optimize reaction kinetics. The reaction products, kinetics, and chemical conditions were studied using both off-chip and on-chip amplification and detection systems. An optimal amplification probe was chosen, and optimal ion concentrations were determined by replacing potassium chloride with potassium acetate. Furthermore, we showed that given these optimized conditions, the initial 65°C step can be eliminated, making the amplification fully isothermal and thus providing significant advantages in field and other point-of-care settings. The hybridization of both a capture and amplifiable probe increases specificity of the assay, and the use of magnetic beads allows for separation of the target-bead complex from unbound amplifiable probe. Our method includes a simple microfluidic reactor to facilitate the separation step. Amplification in wells was shown to have rapid detection at 1 pmol/L and 100 fmol/L with reduced reagent use, requiring only 5 μL of reaction volume. Additionally, the small reaction volume concentrates the target and probe molecules, which may decrease the time to positive. We have also demonstrated capture, on-chip separation, and off-chip amplification. Although evidence existed for nonspecific binding of amplification probe, there was a distinct decrease in signal with endpoint quantification, which corresponds to a large difference in time to positive in real-time quantification for on-chip amplification.

This platform is clinically relevant, given that the probes presented were based on sequences shown to hybridize to full-length influenza A H5 vRNA. Additionally, because of the flexibility of the amplifiable probe sequence, this method can easily be used for detection of any number of RNA targets. The present work thus provides a fundamental basis for a novel and simple general method for RNA detection.

References

1. Thompson WW, Moore MR, Weintraub E, Cheng PY, Jin XP, Bridges CB, Bresee JS, Shay DK: Estimating influenza-associated deaths in the United States. Am J Public Health 2009, 99 Suppl 2:S225–S230
2. Fouchier RA, Munster V, Wallensten A, Bestebroer TM, Herfst S, Smith D, Rimmelzwaan GF, Olsen B, Osterhaus AD: Characterization of a novel influenza A virus hemagglutinin subtype (H16) obtained from black-headed gulls. J Virol 2005, 79:2814–2822
3. Fiore AE, Shay DK, Broder K, Iskander JK, Uyeki TM, Mootrey G, Bresee JS, Cox NS; Centers for Disease Control and Prevention (CDC); Advisory Committee on Immunization Practices (ACIP): Prevention and control of influenza: recommendations of the Advisory Committee on Immunization Practices (ACIP), 2008. MMWR Recomm Rep 2008, 57(RR-7):1–60
4. Beigel JH, Farrar J, Han AM, Hayden FG, Hyer R, de Jong MD, Lochindarat S, Nguyen TK, Nguyen TH, Tran TH, Nicoll A, Touch S, Yuen KY; Writing Committee of the World Health Organization (WHO) Consultation on Human Influenza A/H5: Avian influenza A (H5N1) infection in humans [Erratum appeared in N Engl J Med 2006, 354: 884]. N Engl J Med 2005, 353:1374–1385
5. Writing Committee of the WHO Consultation on Clinical Aspects of Pandemic (H1N1) 2009 Influenza, Bautista E, Chotpitayasunondh T, Gao Z, Harper SA, Shaw M, Uyeki TM, Zaki SR, Hayden FG, Hui DS, Kettner JD, Kumar A, Lim M, Shindo N, Penn C, Nicholson KG: Clinical aspects of pandemic 2009 influenza A (H1N1) virus infection [Erratum appeared in N Engl J Med 2010, 362:2039]. N Engl J Med 2010, 362:1708–1719
6. Mermel LA: Pandemic avian influenza. Lancet Infect Dis 2005, 5:666–667
7. Fauci AS: Pandemic influenza threat and preparedness. Emerg Infect Dis 2006, 12:73–77
8. Germann TC, Kadau K, Longini IM Jr, Macken CA: Mitigation strategies for pandemic influenza in the United States. Proc Natl Acad Sci USA 2006, 103:5935–5940
9. Bonner AB, Monroe KW, Talley LI, Klasner AE, Kimberlin DW: Impact of the rapid diagnosis of influenza on physician decision-making and patient management in the pediatric emergency department: results of a randomized, prospective, controlled trial. Pediatrics 2003, 112:363–367
10. Woo PC, Chiu SS, Seto WH, Peiris M: Cost-effectiveness of rapid diagnosis of viral respiratory tract infections in pediatric patients. J Clin Microbiol 1997, 35:1579–1581
11. Dunn JJ, Gordon C, Kelley C, Carroll KC: Comparison of the Denka-Seiken INFLU A.B.-Quick and BD Directigen Flu A+B kits with direct fluorescent-antibody staining and shell vial culture methods for rapid detection of influenza viruses. J Clin Microbiol 2003, 41:2180–2183
12. Petric M, Comanor L, Petti CA: Role of the laboratory in diagnosis of influenza during seasonal epidemics and potential pandemics. J Infect Dis 2006, 194 Suppl 2:S98–S110
13. Gavin PJ, Thomson RB Jr: Review of rapid diagnostic tests for influenza. Clin Appl Immunol Rev 2004, 4:151–172
14. Dyer Jr, Gilliam BL, Eron JJ Jr, Grosso L, Cohen MS, Fiscus SA: Quantitation of human immunodeficiency virus type 1 RNA in cell free seminal plasma: comparison of NASBA with Amplicor reverse transcription-PCR amplification and correlation with quantitative culture. J Virol Methods 1996, 60:161–170
15. Vandamme AM, Van Dooren S, Kok W, Goubau P, Fransen K, Kievits T, Schmit JC, De Clercq E, Desmyter J: Detection of HIV-1 RNA in plasma and serum samples using the NASBA amplification system compared to RNA-PCR. J Virol Methods 1995, 52:121–132
16. Luebke KJ, Balog RP, Garner HR: Prioritized selection of oligodeoxyribonucleotide probes for efficient hybridization to RNA transcripts. Nucleic Acids Res 2003, 31:750–758
17. Guatelli JC, Whitfield KM, Kwoh DY, Barringer KJ, Richman DD, Gingeras TR: Isothermal, in vitro amplification of nucleic acids by a multienzyme reaction modeled after retroviral replication [Erratum appeared in Proc Natl Acad Sci USA 1990, 87:7797]. Proc Natl Acad Sci USA 1990, 87:1874–1878
18. Deiman B, van Aarle P, Sillekens P: Characteristics and applications of nucleic acid sequence-based amplification (NASBA). Mol Biotechnol 2002, 20:163–179
19. Gulliksen A, Solli L, Karlsen F, Rogne H, Hovig E, Nordstrøm T, Sirevåg R: Real-time nucleic acid sequence-based amplification in nanoliter volumes. Anal Chem 2004, 76:9–14
20. Gulliksen A, Solli LA, Drese KS, Sörensen O, Karlsen F, Rogne H, Hovig E, Sirevåg R: Parallel nanoliter detection of cancer markers using polymer microchips. Lab Chip 2005, 5:416–420
21. Furuberg L, Mielnik M, Gulliksen A, Solli L, Johansen IR, Voitel J, Baier T, Riegger L, Karlsen F: RNA amplification chip with parallel microchannels and droplet positioning using capillary valves. Microsyst Technol 2008, 14:673–681
22. Dimov IK, Garcia-Cordero JL, O'Grady J, Poulsen CR, Viguier C, Kent L, Daly P, Lincoln B, Maher M, O'Kennedy R, Smith TJ, Ricco AJ, Lee LP: Integrated microfluidic tmRNA purification and real-time NASBA device for molecular diagnostics. Lab Chip 2008, 8:2071–2078
23. Kerby MB, Freeman S, Prachanronarong K, Artenstein AW, Opal SM, Tripathi A: Direct sequence detection of structured H5 influenza viral RNA. J Mol Diagn 2008, 10:225–235
24. Kern JA, Davis RH: Application of solution equilibrium analysis to in vitro RNA transcription. Biotechnol Prog 1997, 13:747–756
25. Prakash AR, Amrein M, Kaler KVIS: Characteristics and impact of Taq enzyme adsorption on surfaces in microfluidic devices. Microfluid Nanofluidics 2008, 4:295–305
26. Beverung CJ, Radke CJ, Blanch HW: Protein adsorption at the oil/water interface: characterization of adsorption kinetics by dynamic interfacial tension measurements. Biophys Chem 1999, 81:59–80